University of
Sistan and Baluchestan

Iranian Journal of Archaeological Studies

Print ISSN: 2251-743X Online ISSN: 2676-2919

Archaeological Sciences
Research Centre

Spatial and Quantitative Analyses of Sasanian Ceramics from the Architectural Spaces of Bazeh-Hur *Chahartaq*

Meysam Labbaf-Khaniki[*, 1], Maria Daghmehchi [1], Alfredo Maximiano Castillejo[2], Mehdi Samadi[3] and Afshin Fayyaz Movaghar[4]

[*]*Corresponding Author,* [1]*Department of Archaeology, University of Tehran, Iran.*
E-mail: labbaf@ut.ac.ir

[2]*Quantitative Archaeology Lab, Departament de Prehistòria, Universitat Autònoma de Barcelona, Spain.*

[3]*Department of Remote sensing and GIS, Faculty of Geography, University of Tehran, Tehran, Iran.*

[4]*Department of Statistics, University of Mazandaran, Iran.*

Received: 05/ 09/ 2018; Received in Revised form: 01/ 12/ 2018; Accepted: 28/ 12/ 2018

Abstract

This study presents a model for the spatial structure of ceramic vessels across the architectural complex of Bazeh-Hur site (6th to 8th centuries AD), using Inverse Distance Weighting interpolation for modelling and Mean Relative Error and Root Mean Square Error for validation and cross-validation of the output modelled surface. The Regression analysis was also used to examine the vessel prediction per square meter and measure the correlation intensity between the values and distance. These geostatistical and quantitative methods not only enable us to characterize the arrangement of the architectural spaces where activities take place, but also to delimit several structures that are corroborated by the excavated areas. As a conclusion, we propose a high probability for the main entrance of the building in southern *taq*, which is also attested by a chief portico and a broad gypsum floor near to an ancient trade road.

Keywords: Inverse Distance Weighting; Regression Analysis; Validation; Ceramics; Bazeh-Hur.

Article Type: Research Article

Introduction

The building of Bazeh-Hur in north-eastern Iran has a characteristic plan, typically known as *chahartaq* (see Huff and O'Kane 1990). It was designed with a specific plan, however, the poor preservation of the main building and its surrounding associated structures makes it difficult to associate it with a specific function. Many scholars stated that it may have been used as a defensive installation or as a fire temple (Reuther 1938: 552; Godard 1938: 53ff; Herzfeld 1942: 33; Wilber 1946: 27-28). In the present research, predictive modelling along with archaeological excavations are implemented to assess the potential function of the main building.

Predictive modelling can be used to recognize some aspects of the past human activities and behaviour that occurred in specific spaces, then spatial models applied at intra-site scale enable us to determine activity areas (Achino and Barceló 2018: 1). In order to proceed, spatial modelling by interpolation techniques in Geographic Information Systems (GIS) provides a powerful tool to predict values (Huang *et al.* 2011: 428; Gong *et al.* 2014: 59; Maximiano *et al.* 2018: 679). In this study, Inverse

© The Author(s):

DOI: 10.22111/IJAS.2019.6507

Publisher: University of Sistan and Baluchestan

Distance Weighting (IDW) interpolation method has been chosen for map prediction as the correlation coefficient between measured and estimated values is greater with IDW than other interpolations (Gong *et al.* 2014: 59). Additionally, IDW trend is very useful to reveal activities in small scale areas such as single rooms of buildings and inner versus outer space (Pecci *et al.* 2013: 887; Rondelli *et al.* 2014: 487). This way, interpolation of known values from the site's surface was initially used to determine the limits of structures; then, the predicted model of superficial pottery enabled us to excavate the most probable locations for structures where pots were buried deep below the main construction. Due to the limited extension of excavation and the presence of a high quantity of pottery in lower layers, it is not possible to measure the whole extent of the site during the Sasanian period.

Nonetheless, predictive modelling provides a useful method to characterize the probability of pottery distribution in the site. Furthermore, the quality assessment of the predicted model is calculated by omitting a subset of data from model generation and keeping it for further testing. Then, Mean Relative Error (MRE) and Root Mean Square Error (RMSE) statistics were calculated during cross-validation to estimate the accuracy of the interpolation (Gong *et al*. 2014: 67; Xu *et al*. 2015: 170; Ogundimu *et al*. 2016: 6), and the obtained weighted values are used to measure the accuracy of the interpolation of different vessel forms at specific places.

Study Area And Archaeological Research

The ancient site of Bazeh-Hur is located about 75km south-west of the modern city of Mashad, in north-eastern Iran, 3 km south-west of the modern village of Ribat-e Sefid. The defence system of Qale-Dokhtar fortress, with similar chronology, as well as an ancient trade route in the south part of the site, showed the significant importance of the site in the Sasanian period (224-651 AD) and established a specific landscape in this area (Figure. 1).

Previous studies conducted by Ernst Herzfeld (1942), Oscar Reuther (1938), Donald Newton Wilber (1946), and André Godard (1938) provide some contextual information about the visible parts of the structure, including plans where doubts

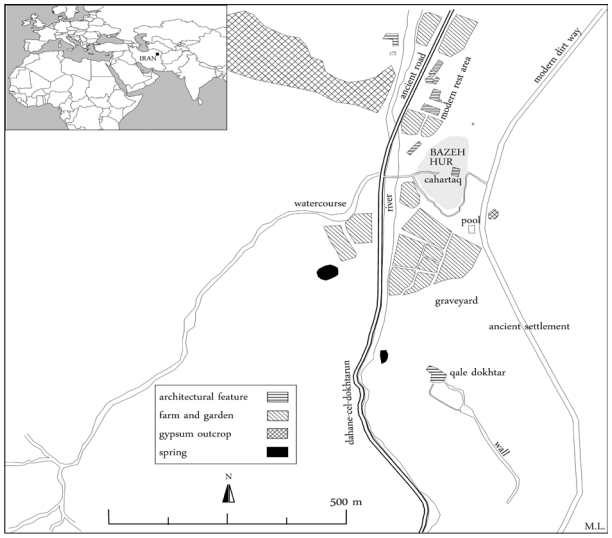


Figure. 1*: Location of the Bazeh-Hur chahartaq and the landscape of Bazeh-Hur valley (Drawn by M. Labaf-Khaniki).*

on some structures were represented as hatched blocks (Figure. 2). In order to recognise the form and function of the complex, the archaeological investigations carried out in 2014 revealed some architectural remains related to the adjoining rooms surrounding the central massive *chahartaq* (Figure. 3). Twenty-two trenches were opened in Bazeh-Hur: six in the south of the site (1x1 m), and sixteen in the area of the *chahartaq*, where five of them, both inside and outside of the *chahartaq*, exposed some architectural features of the building such as walls, floors, doorways, columns, and rooms (Labbaf-Khaniki 2017: 259). Three lateral, surrounding spaces to the central *chahartaq* were discovered along with two narrow corridors in the northern and southern sides, as well as a columned hall to the east. The dig also revealed that the western and eastern *taqs* of the main building was once blocked by a north-south oriented wall. The excavated structures represent equivalent annexes on the southern and northern sides (Labbaf-Khaniki 2017: 261). Moreover, excavation and systematic survey on the site provided a collection of 1800 pottery sherds from both, Late Sasanian and Early Islamic periods. The cream-coloured wares were considerably frequent in the ceramic assemblage due to the high frequency of the Ca phase of the raw material mixture (Hai-tao *et al.* 2015: 258; Daghmehchi *et al.* 2018:148).

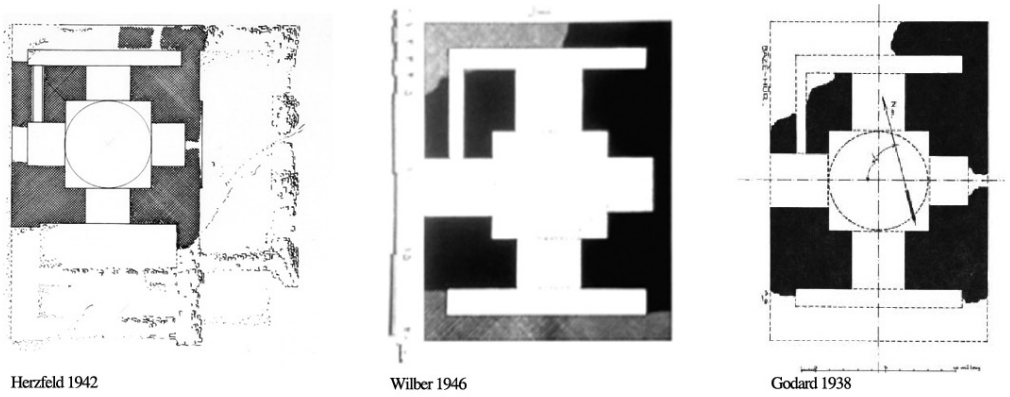


Figure. 2: *Three plans of the Bazeh-Hur chahartaq provided by Herzfeld (1942), Wilber (1946), and Godard (1938) show some ambiguous structures surrounding the central building.*



Figure. 3: *A general view of the Bazeh-Hur chahartaq from the north-east and remains of the adjoining rooms. (Photographed by Meysam Labbaf-Khaniki).*

Predictive Modelling

Inverse Distance Weighting

The IDW interpolation models a continuous distribution of cultural and geographical data (Bevan and Conolly 2009: 958). Inverse Distance Weighting (IDW) is a technique to estimate unknown values by interpolating the measured ones as a weighted function of both, a known sample in a certain place and the distance between that known sample and other unknown places (Luo and Wei 2009: 180; Huang *et al*. 2011: 428; Gong *et al.* 2014: 60; Ivajnsic *et al.* 2014: 341); hence, measured points with a high amount of ancient remains have greater weights.

To provide an input for the IDW model, ceramic remains were sampled at 110 control points around the main building, in a series of 5x5 m squares distributed over 1200 sq. m throughout the site; this model will serve to examine the distribution of different vessel forms on the output modelled surface. As the vessel brokenness can highly influence the weighting function for the collected values, pots from each grid were initially estimated by a minimum number of individuals (MNI) to minimize the brokenness factor throughout the site and to increase the accuracy of interpolation (Starck 2008: 4; Voss and Allen 2010: 3). This approach also enables us to estimate the proportion of complete types around the main building in the same chronological contexts. This way, once ceramic assemblages were quantified with IDW to determine the spatial variation of pottery distribution, the results were then confirmed by excavating the area in the vicinity of spatial concentrations of remains to verify the activity area.

The interpolation-estimated values are influenced by the observed values at the measured points and can be represented by the following equation (Huang *et al.* 2011: 428):

$$Z = \frac{\sum_{i}^{n}=1\ w_i z_i}{\sum_{i}^{n}=1\ w_i} = \frac{\sum_{i}^{n}=1\ Z_i / D_i^p}{\sum_{i}^{n}=1\ 1/D_i^p}$$

Where Z is the interpolated value which is influenced by the known values (Zi) at control point i, Wi the weighting function that determines the relative importance of the observed value in each data point and n is the total number of observed control

points in the interpolation, and Dpi is the distance from the observed control point i to the interpolated point, where p is the weighting exponent (Huang *et al*. 2011:428). The known values (Z_i) provide a statistical description of various types of ceramics and small finds in the measured point i, quantifying the local variation. Although the estimated model with IDW shows that the more distant is a known point to the unknown points, the less influence it has on the prediction (Chen *et al.* 2017: 19), that influence can be managed by weighting the measurements at known points with a power (Conolly and Lake 2006: 96; Chen *et al.* 2017: 19). The high power value ($p = 2$) which is used as a default value, may generate the predicted location at the immediate surrounding points (Esri, 1995-2014). Finally, the modelled values represented in the predicted maps can be expressed as the proportion of specific types and small finds.

The interpolation-estimated values surrounding the observed control points show different distribution patterns of vessel forms near the building (Figure. 4). Interpolation-estimated values are closely correlated with the measured values (Gong *et al.* 2014: 61), and the optimal power value generated certain points of the predicted pots and bowls at the immediate surrounding points.

The spatial structure of different types of vessels need to be validated by field data. As the interpolation of the vessel forms may change due to the functional difference of architectural spaces, a systematic survey was carried out and various types of jars were well documented in the south part of the central building, however that vessel type was highly absent in eastern and western part of the central building. The concentration of specific ceramic types associated with the determinate location was highly demonstrated by architectural structures and the main doorway in the vicinity of spatial concentrations. The archaeological excavation indicates a spatial structure distribution around the main building. Some architectural features including long and narrow rooms had been found in both the southern and northern sides of *chahartaq*, contemporaneous to the main building. However, the excavation also revealed a hypostyle room with two rows of columns on the eastern side of the *chahartaq* (Figure. 5). The occurrence of different forms of architectural spaces and doorways in the vicinity of the main building indicates the activity area with determinate ceramic types. The excavation in the western side represented a wall blocking the western portico of the *chahartaq* which is similar to the eastern *taq* wall. The lack of architectural structures in the tranches from the western side of *chahartaq* also confirms the low probability of the spatial distribution of ceramics in this area. Additionally, the ceramic types were largely absent in the hypostyle room in the eastern part of the main building, revealed by both trend-surface analysis and the excavated areas. However, the trend-surface analysis shows a high concentration of various types of jars near the southern *taq*, and suggests a high probability of the presence of architectural structures in the south part of the main building. The excavation conducted in the southern part of the *chahartaq* supported that inference, and these structures could be related to the main building. The trenches uncovered a lateral corridor 1.60 m in width, parallel to the southern wall of the *chahartaq* (Plan.1), but the southern wall of the corridor was cut by a doorway and overlooked directly the ancient trade route passing beside the site and the fortress (Qaleh-Dokhtar), situated on the summit of the southern mound. The doorway was more likely to be the main entrance to the central building and can be considered as the chief portico (*ivan*). The trenches near to that *ivan* also revealed various types of jars with no uniformity in size; these specific types were found in high fragmentation with the leaching of gypsum due to use and consequently showing the same depositional history (Orton *et al.* 2007: 215; [Figure. 6]). The occurrence of gypsum in building materials and on the outer surface of different types of the jars which were found in the structural spaces, may distinguish the activity area from waste. According to Orton *et al*. (2007:28) 'variation in the proportion of different types, may indicate areas of different functions or status'. The excavated ceramics from the intra-space of the building and on the gypsum floor of the southern *ivan* revealed the same depositional history contemporaneous to the last activity that occurred in the space. The extensive excavation revealed no architectural space at further parts of the central building. The lateral corridors and the hypostyle room linked to the eastern part of the central building make it possible a unique entity in the Sasanian period. The

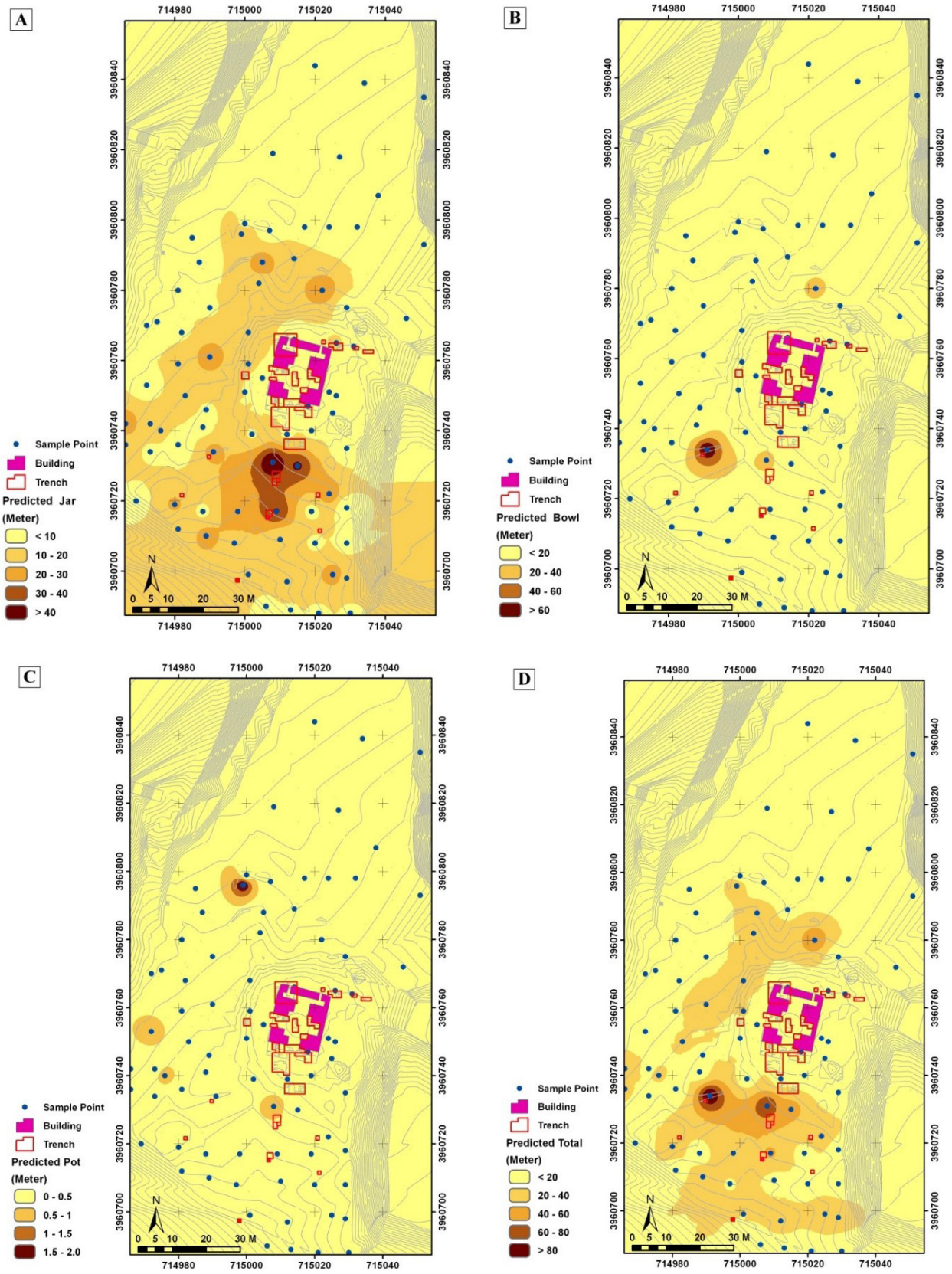


Figure. 4: *Predictive map of the spatial distribution of vessels estimated by IDW interpolation. (Produced by Maria Daghmehchi).*

excavated ceramics also indicated a spatial variation surrounding the main building. However, the lack of *in situ* features and very low quantity of ceramic sherds inside the building do not necessarily imply domestic spaces, and the concentration of various jars in the chief portico and the lateral corridor in the north may imply a possible public function of the building near the trade road. Nonetheless, the ceramic concentration in the measured location at farther apart did not support any evidence of a possible spatial structure. Thus, a random distribution may generate certain points of spatial concentration of the evidence with greater weights around the building. The excavation conducted at the measured and predicted locations revealed that the concentration of evidence does not condition a determinate type of activity space. The trade road which was considered as the main transmission network in eastern Iran (Afzal-al Molk 1903: 128ff) and the fortress (Qale-Dokhtar) in the southern part of the building had more influence on the ceramic expansion in the southern *taq*. The petrographic and typological studies of the ceramics from the fortress and Baze-Hur building indicated a great association between the sites (Daghmehchi 2018: 19).

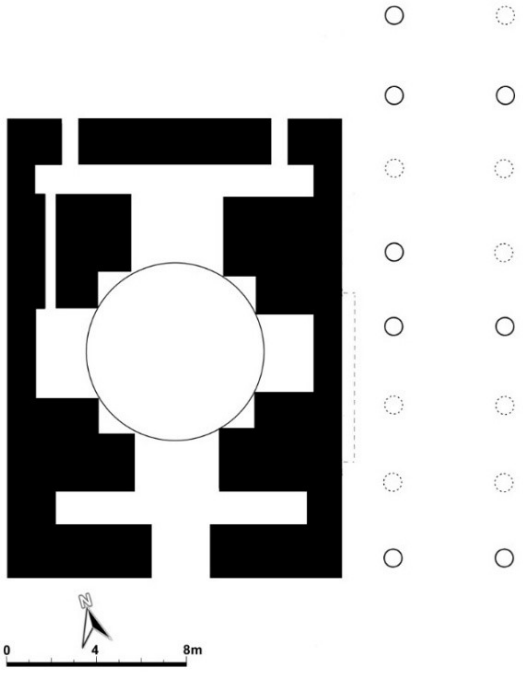


Figure. 5: *The final plan of Bazeh-Hur chahartaq, showing the hypostyle room with two rows of columns and some unexcavated columns in dotted line. (Drawn by Meysam Labbaf-Khaniki).*

Estimation of the prediction accuracy

The accuracy of models was obtained using cross-validation and validation. In order to validate the output modelled surface, predicted values need to be compared against the measured values that were not involved in interpolation (Esri 2014); this way, the dataset is divided into two parts with 'subset features tool', one for training and other for testing. Initially, 20 sampling points were separated for testing and the training subset was interpolated at the rest of the locations. We eventually summarized the values of the test dataset using the remaining subset through zonal statistics to compare the predicted values to the actual values at the omitted points. The statistic type is defined by maximum, mean and standard deviation.

The cross-validation also compares the measured and predicted values at the omitted data location. For IDW only the mean relative error (MRE) and root mean square error (RMSE) of the interpolated values estimate the accuracy of the interpolation-estimated values in the surface by determining an optimal power value and calculated with the following equations (Gong *et al.* 2014: 61; Ogundimu *et al*. 2016: 6):

$$MRE = \frac{1}{n}\sum_{i=1}^{n}\left|\frac{Z_m(X_i) - Z_i(X_i)}{Z_m(X_i)}\right|$$

$$RMSE = \sqrt{\frac{1}{n}\sum_{i=1}^{n}(\hat{y}_i - y_i)^2}$$

where $Z_m(X_i)$ and y_i are the measured values and $Z_i(X_i)$ and $y_i\hat{}$ are the predicted values, and n is the total number of predicted steps (Gong *et al.* 2014: 61; Zheng *et al.* 2016: 98).

The weighting values show a significant variation of vessel forms concentrations through the surface. Statistic comparison of the mean and standard deviation of ceramics show the highest concentration of jar and the lowest concentration of coarse fabric pots (Table 1). The spatial structure of cooking pots shows the very small root mean square error only due to the very small values of this vessel form. The scatter plot shows an over prediction of the small values (Esri 2014; Figure.

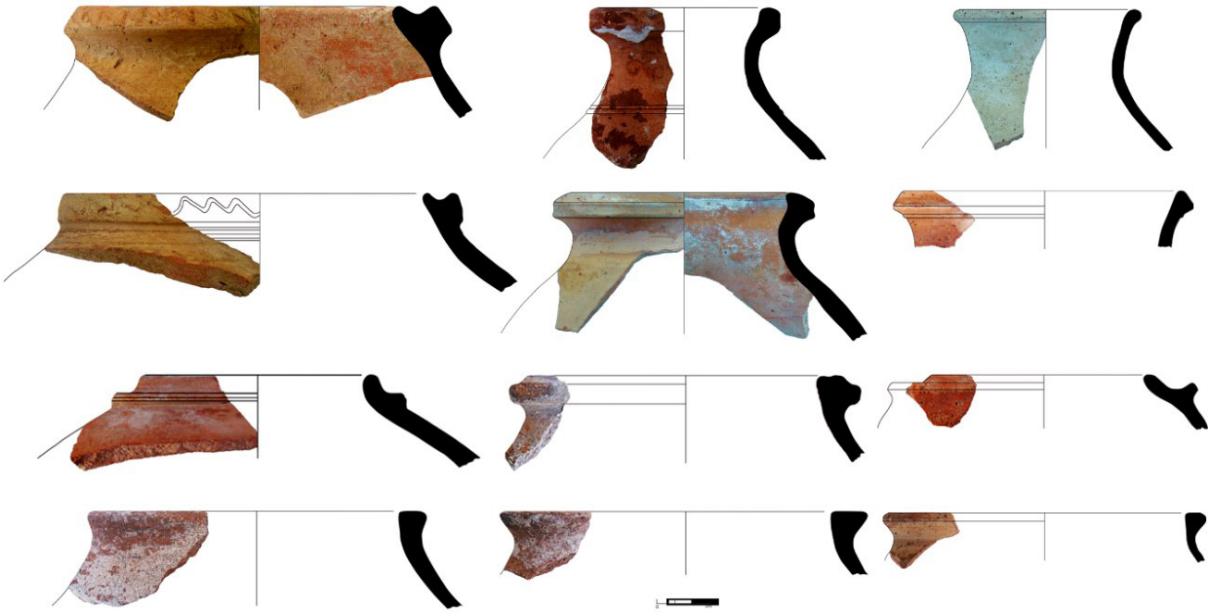


Figure. 6: *Various types of jars from the southern taq. (Drawings and Photographs by Maria Daghmehchi).*

7). A small mean relative error and the small root mean square error of bowls indicate a more valid prediction model and a better surface possible. The scatterplot of the bowl falls relatively close to the 1:1 line. However, the high root mean square error of jars indicated a comparatively low quality of the output surface. The slope of jars that are scattered around the 1:1 line is more than 5.

The spatial structure of jars obtained the highest RMSE and MRE due to different anomalies. Therefore, the spatial concentration of a specific type of jar does not condition the space but is a part of extensive relations that occur in space. This result was accomplished by comparison with the archaeological excavations: trenches 10, 13 and 17 in the southwestern part of the building revealed the concentration of glazed bowls at the latest occupational deposit (Early Islamic). However, the Sasanian jars were highly distributed in the chief southern portico and the lateral corridor in the north, all found at the same depositional history. The occurrence of the jars from the north part of the building was only verified by two small doorways. The specific spatial structure of jars in the southern chief portico can be related to the geographical location of the *chahartaq* near the ancient trade road and a caravanserai along the road.

The best regression line

Quantitative approaches such as regression analyses estimate the known values (measured ceramics) as the response variable, while IDW estimates explanatory variables included predicted vessels (Gong *et al*. 2014: 61). Regression analyses provide an effective means to examine the correlation between the predicted size and the measured size and increase significantly the accuracy of the interpolation. This method enables us to clarify how well the ceramic distribution is predicted and is an effective method for the prediction of the distribution of unknown sample size by the measured sample size per square meter.

The best regression line is a line that has the least-squares of residuals (Niknami 2008: 227). The least-square criterion method contributes to predicting unknown vessel count by the measured vessel within the identified radius. For finding the best regression line, we need to estimate the parameter of intercept (a) and slope (b) as the following quantification (Niknami 2008: 227; Spiegel *et al*. 2009: 105):

$$b = \frac{\mathrm{n}\left(\sum_{\mathrm{i}=1}^{\mathrm{n}} x_i y_i\right) - \left(\sum_{i=1}^{n} x_i\right)\left(\sum_{i=1}^{n} y_i\right)}{\mathrm{n}\left(\sum_{\mathrm{i}=1}^{\mathrm{n}} x_i^2\right) - \left(\sum_{i=1}^{n} x_i\right)^2}$$

$$a = \frac{\sum_{\mathrm{i}=1}^{\mathrm{n}} y_i - b\sum_{i=1}^{n} x_i}{\mathrm{n}} = \frac{\sum_{i=1}^{n} y_i}{n} - b\frac{\sum_{i=1}^{n} x_i}{n} = \overline{y} - b\overline{x}$$

Where x_i is the analyzed area (in square meters) and y_i is the observed number of vessels estimated by MNI and n is the total control points, and then determine the line (y =a+bx).

The mathematical quantification shows that 3.15 + 0.1376 vessels might be found per sq. meter. Therefore, the predicted number of sherds within the analysed area (in sq. m) is 1697.694 sherds, as Y=3.15+(0.1376)(12315)=1697.694, while the observed number of sherds is 2150; then, there is a deviation of 452 sherds between the observed and predicted sherds as a residual that remains unpredicted through the regression line.

Coefficient of determination or r^2 contributes to measuring the correlation intensity of the linear relationship between predicted and observed values

Table 1: *The statistical description of the vessel forms*

Vessel From	Max	Mean	STD	RMSE	MRE
Jar	53	11.075	11.011	11.950	1.833
Bowl	77	5.392	9.548	3.661	1.023
Pot	2	0.063	0.290	0.260	0.904
Total	101	16.531	17.476	14.946	3.432

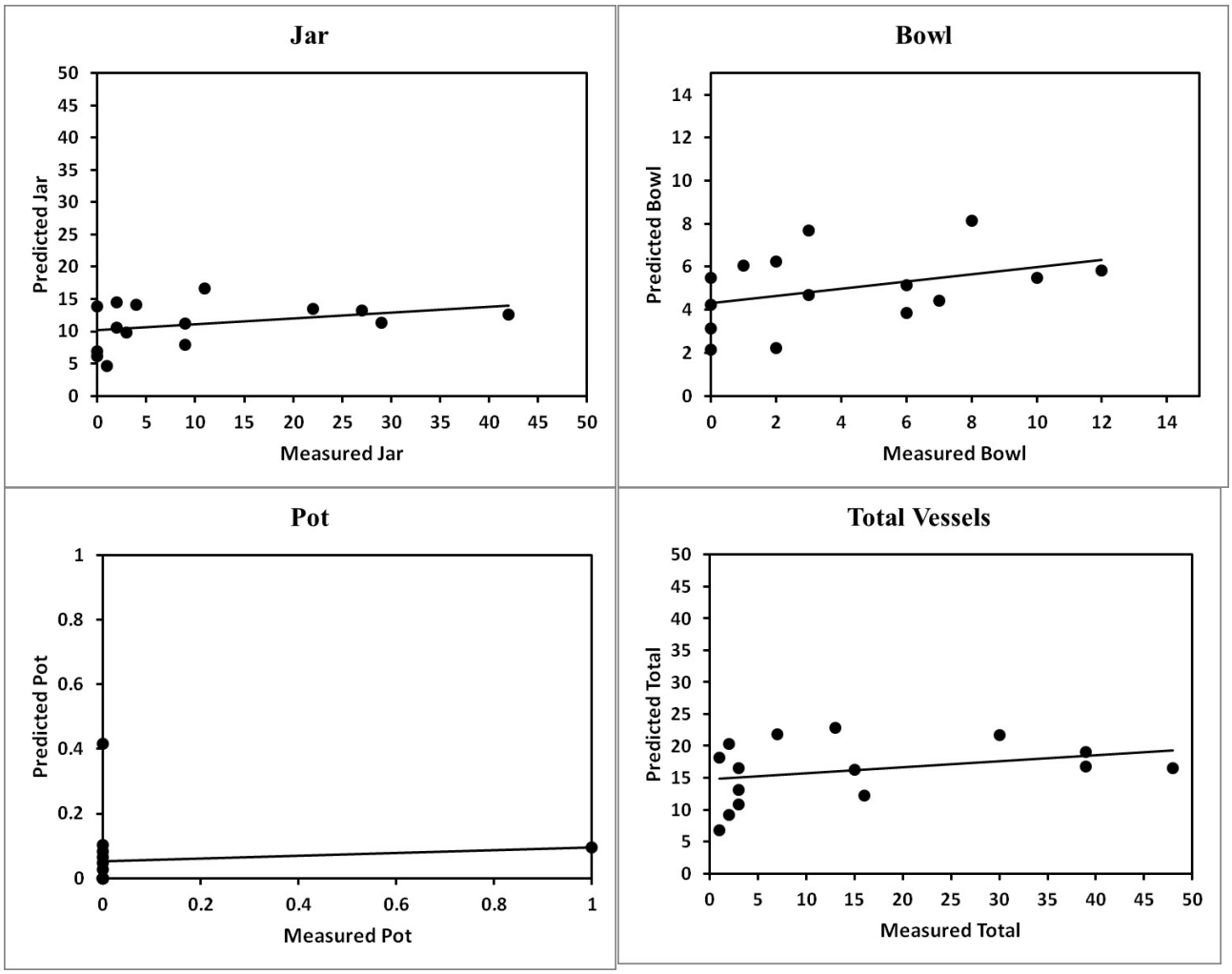


Figure. 7: *Scatterplots showing the predicted values versus the actual values. (Produced by Maria Daghmehchi).*

(Xu *et al.* 2015: 169; Sung *et al.* 2016: 1028). Deviation value of y from $\bar{y}$ has been estimated with the following equation:

$$y - \bar{y} = (y_i - \hat{y}) + (\hat{y} - \bar{y})$$

y_i-$\hat{y}$ is an error which is not being represented by the regression line while $\hat{y}$-$\bar{y}$ is an error which is represented by the regression line (Niknami 2008: 236).

$$\sum_{i=1}^{n}(y_i - \bar{y})^2 = \sum_{i=1}^{n}(y_i - \hat{y})^2 + \sum_{i=1}^{n}(\hat{y} - \bar{y})^2$$

Therefore, r^2 can be calculated by the following equation (Xu *et al.* 2015: 169):

$$r^2 = \frac{\Sigma(\hat{y} - \bar{y})^2}{\Sigma(y_i - \bar{y})^2} = \frac{84.66}{86} = 0.98$$

r^2 equation shows that 98% of observed changes in vessel count by the excavation and surface volume are being represented by the linear relationship. The r^2 equation indicates a high accuracy of $\hat{y}$ at different distances.

Conclusion

The combination of predictive modelling and quantitative measurement contributes to accurately predicting the spatial structure of the ceramic sherds on the site's surface, which were related to the main building of Bazeh-Hur. The interpolation-estimated values indicated a continuous distribution of pottery with different patterns, and the validation result implies extensive relations between the spatial distributions and the building.

The existence of the blocked *taqs* highlighted no spatial distribution of pottery in the eastern and western parts of the main building. However, the high concentration of various jars in the chief southern portico and the lateral corridor in the north can be related to its association with the road.
The high amount of jars identifies some aspects of the function of the construction: the form of the jar was commonly used as a vessel for transferring goods or liquids by users who have decided not to dwell for a long time at a particular place. As this activity can occur in spaces that serve as public buildings but not as permanent residences for a particular group of people, the *chahartaq* of Bazeh-Hur is proposed to be a public building from the Sassanid period in close relation to the fortress and the ancient trade route.

Acknowledgement

We would like to thank the anonymous referees constructive comments. The research is financially supported by the Cultural Heritage, Tourism and Handicraft Office of Khorasan-e Razavi province. We are grateful to Seyyed Mohammad Beheshti, then director of the Research Institute of Cultural Heritage & Tourism, Hamideh Choubak, then director of the Iranian Center for Archaeological Research, and Rajabali Labbaf-Khaniki then director of the Cultural Heritage, Tourism and Handicraft Office of Khorasan-e Razavi province for their support of our work. The authors would also like to thank M. Rokni, M. Toghraei, A. Shahmohammadpour, M. Malekzadeh, M. Gholinezhad, A. Mottaghi, M. Abdollahzadeh, H. Soleymani, I. Beheshti, N. Tabatabaei, and K.

References

Afzal al-Molk, Gh. 1903. *Safarname-ye Khorasan va Kerman (The Book of Travels to Khorasan and Kerman),* edited by Gh. Roshani Zaferanlou, Tous Publishing, Tehran. (in Persian)

Bevan, A. & J. Conolly, 2009. Modelling spatial heterogeneity and nonstationarity in artifact-rich landscapes, *Journal of Archaeological Science* 36, 956–964.

Clarkson, C. & A. Bellas, 2014. Mapping stone: using GIS spatial modelling to predict lithic source zones, *Journal of Archaeological Science* 46, 324-333.

Conolly, J. & M. Lake, 2006. *GIS and archaeology*, Cambridge University Press, Cambridge.

Daghmehchi, M.; H. Omrani; M. Emami, J. Nokandeh 2016. Mineralogical and thermo-chemical characteristics of the Hellenistic ceramics and raw clay from Qizlar Qal'eh (northeastern Iran), *Materials Characterization* 120, 143–151.

Esri, 2012. *An Overview of the Interpolation Toolset*. http://help.arcgis.com/en/ arcgisdesktop/10.0/ help/index.

Ghafoorian, R.; H. Sanaie Nejad; A. Dadrasi & J. Ezi, 2012. Arzyabi ravesh-haye Taeen Shib dar yek Hoze Abkhiz (Analysing the Methods of Estimating Mean Watershed Slope). *J. of Eng. and Watershed Managing*, 1/3, 57-66.

Godard, A. 1938. *Athar-e Iran III*, Librairie Orientaliste Paul Geuthner, Paris.

Gong, G.; S. Mattevada & S. E. O'Bryant, 2014. Comparison of the accuracy of kriging and IDW interpolations in estimating groundwater arsenic concentrations in Texas. *Environ. Res*, 130, 59–69.

Hai-tao, W.; K. Ling-xue; B. Jin; B. Zong-qing; L. Dong-mei & L. Wen, 2015. Transformation of minerals in direct coal liquefaction residue under gasification atmosphere at high temperatures, *Journal of fuel chemistry and technology* 43 (3), 257-65.

Herzfeld, E. 1942. Damascus: Studies in Architecture. *Ars Islamica* 9, 1-53.

Huang, F.; D. Liu; X. Tan; J. Wang, Y. Chen & B. He, 2011. Explorations of the implementation of a parallel IDW interpolation algorithm in a Linux cluster-based parallel GIS. *Computers and Geosci*, 37, 426–434.

Huff, D. & B. O'Kane, 1990. Čahārtāq, in: Yarshater, E. (Ed.), *Encyclopaedia Iranica*, vol. IV. Mazda Publishers, California, pp. 634-642.

Ivajnsic, D.; M. Kaligaric & I. Ziberna, 2014. Geographically weighted regression of the urban heat island of a small city. *Appl. Geogr*, 53, 341-353.

Luo, J. & Y. H. D Wei, 2009. Modeling spatial variations of urban growth patterns in Chinese cities: The case of Nanjing. *Landsc. and Urban Plan*, 91, 51–64.

Mickey, R. M. 2003. *Applied Statistics, Analysis of Variance and Regression*, Wiley, New York.

Niknami, K. 2008. *Quantitative Methods in Archaeological Researches*, (In Persian), Vol.1: Basic Methods. Samt Publishing, Tehran.

Ogundimu, E.O.; D. G. Altman & G. S. Collins 2016. Adequate sample size for developing prediction models is not simply related to events per variable, Journal of Clinical Epidemiology, in press.

Orton, C. & M. Hughes, 1993. *Pottery in Archaeology*, Cambridge University Press, Cambridge.

Papachristodoulou, C.; A. Oikonomou, ; K. Ioannides & K. Gravani, 2006. A study of ancient pottery by means of X-ray fluorescence spectroscopy multivariate statistics and mineralogical analysis, *Analytica Chimica Acta*, 573–574, 347–53.

Reuter, O. 1938. Sasanian Architecture, in Pope, A. (Ed.), *A Survey of Persian Art, Sasanian Art*, Vol.1, (493-578). Oxford University Press: Oxford.

Spiegel, M.R.; J.J. Schiller; R.A. Srinivasan; M. Le Van, 2009. *Probability and Statistics*. McGraw-Hill, New York.

Starck, S. 2008. Erfahrungsbericht' of Application of Different Quantitative Methods at Kalapodi, in: Verdan, S., Theurillat, T., Kenzelmann Pfyffer A. (Eds.), *Early Iron Age Pottery: A Quantitative Approach* (45-60), (Proceedings of the International Round Table organized by the Swiss School of Archaeology in Greece, Athens.

Sung, M. C.; D. C. J. Mc Donald & J. E. V. Johnson, 2016. Probabilistic forecasting with discrete choice models: Evaluating predictions with pseudo-coefficients of determination, *European Journal of Operational Research*, 248, 1021–1030.

Voss, B.L. & R. Allen, 2010. Guide to Ceramic MNV Calculation Qualitative and Quantitative analysis. *Tech. Briefs in Hist. Archaeol*, 5, 1-9.

Wackerly, D.; W. Mendenhall & R. Scheaffer, 2008. Mathematical Statistics with Applications, Seventh ed.Thomson Brooks, California.

Wilber, D. N. 1946. The Ruins at Rabat-i-Safid, *Bulletin of the Iranian Institute*, 6-7, 22-28.

Xu, L.; Y. Cheng; R. Yin & Q. Zhang, 2015. Comparative study of regression modeling methods for online coal calorific value prediction from flame radiation features. *Fuel*, 142, 164–172.

Yang, Ch. 2016. Correlation coefficient evaluation for the fuzzy interval data. *J. Bus. Rese*, 69, 2138-2144.

Zheng, L.; Z. Jun; L. Ying & W. Wei, 2016. Use of a quintile regression based echo state network ensemble for construction of prediction Intervals of gas flow in a blast furnace. *Control Eng. Pract*, 46, 94-104.

Labbaf-Khaniki, M. 2017. Excavations at Bazeh-Hur in North-Eastern Iran: A Preliminary Report, *Iran*, 55 (2), 253–270.

Wei-Hsin Chen, Hung-Jen Hsub, Gopalakrishnan Kumar, Wojciech M. Budzianowskid & Hwai Chyuan Ong. 2017. Predictions of biochar production and torrefaction performance from sugarcane bagasse using interpolation and regression analysis, *Bioresource Technology*, 246, 12–19.

Achino, A. F. & J. A. Barceló, 2018. Spatial Prediction: Reconstructing the spatiality of Social Activities at the Intra-Site Scale. *J Archaeol Method Theory*, 1-23.

Alessandra Pecci; Miguel Ángel Cau Ontiveros & Chiara Valdambrini. 2013. Fernanda Inserra Understanding residues of oil production: chemical analyses of floors in traditional mills, *Journal of Archaeological Science* 40, 883-893.

Bernardo Rondelli; Carla Lancelotti; Marco Madella; Alessandra Pecci; Andrea Balbo; Javier Ruiz Pérez; Fernanda Inserra; Charusmita Gadekar; Miquel Ángel Cau Ontiveros & P. Ajithprasad, 2014. Anthropic activity markers and spatial variability: an ethnoarchaeological experiment in a domestic unit of Northern Gujarat (India), *Journal of Archaeological Science* 41, 482-492.

Alfredo Maximiano Castillejo; Facundo Gómez Romero; Carlos Landa & Camilo Barcia García, 2018, Archaeological spatial analysis and GIS in a small fortification: Ephemeral occupations along the border during the 'Conquest of Desert' process in Argentinean Pampas (19th Century), *Journal of Archaeological Science:* Reports 18, 679-688.